Journal of Carcinogenesis
Covering Genesis to Therapeutics

Journal of Carcinogenesis, ISSN: 1477-3163
2025; Vol 24: Issue 2s, https://carcinogenesis.com/

Characterization And Bioactivity of Nanohydroxyapatite-Gelatin Paste as A Scaffold Using Simulated Body Fluid

Viona Yosefa[1], Maria Savvyana Saputra[1], Nadhia Anindhita Harsas[2], Fatimah Maria Tadjoedin[2], Natalina Haerani[2], Basril Abbas[3], Cortino Sukotjo[4], Endang W. Bachtiar[5], Yuniarti Soeroso[2*]

[1]Specialist Program in Periodontology, Faculty of Dentistry, Universitas Indonesia, Jakarta, Indonesia

[2]Department of Periodontology, Faculty of Dentistry, Universitas Indonesia, Jakarta, Indonesia

[3]National Research and Innovation Agency (BRIN) Jakarta, Indonesia

[4]Department of Prosthodontics, University of Pittsburgh, Pennsylvania, United States

[5]Department of Oral Biology, Faculty of Dentistry, Universitas Indonesia, Jakarta, Indonesia

Email ID: vionaodiliadv@gmail.com / Email ID: mariasavvyana@gmail.com / Email ID: nadhia.anindhita02@ui.ac.id

Email ID: Fatimah.tadjoedin@ui.ac.id / Email ID: natalina_perio@ui.ac.id / Email ID: basr001@brin.go.id

Email ID: csukotjo@uic.edu / Email ID: endang04@ui.ac.id / Email ID: yuniarti_22@yahoo.co.id

***Corresponding Author:**

Yuniarti Soeroso

Email ID: yuniartisoeroso22@gmail.com

ABSTRACT

Objective: Assess the bioactivity of nanohydroxyapatite gelatin paste as a scaffold using simulated body fluid, which used to treat irregular bone defects in bone regeneration therapy and to make the bone graft placement easier during surgery.

Methods: nHA paste was prepared in this study by combining bovine-derived nHA-gelatin with hydroxypropyl methylcellulose (HPMC) at various concentrations. The nHA/G 65/35 and 60/40 pastes were immersed in SBF for 1, 2, 7, and 14 days.

Results: The highest degradation was found on day 7 in both pastes, with the most optimal swelling up to day 14, while pH revealed a significant difference except on day 2. The TEM test showed particles of nHA have an average length of 181.7 ± 20.3 nm and a diameter of 26.9 ± 1.9 nm. After immersion, FTIR demonstrated that the paste hydrolyzed as the O-H functional group and PO_4^{3-} increased. SEM and EDS testing revealed that nHA/G 65/35 had a larger pore size and the highest Ca-P composition. Cell viability showed both pastes indicating nontoxic properties.

Conclusions: the nHA/G 65/35 paste is the best candidate for use as a scaffold due to its superior bioactivity in terms of degradability, pH, and physical, and chemical properties.

Keywords: *Biomaterial, Bone regenerative therapy, Nanohydroxyapatite, Simulated body fluid, Regenerative Periodontal Treatment.*

How to Cite: Viona Yosefa, Maria Savvyana Saputra, Nadhia Anindhita Harsas, Fatimah Maria Tadjoedin, Natalina Haerani, Basril Abbas, Cortino Sukotjo, Endang W. Bachtiar, Yuniarti Soeroso, (2025) Characterization And Bioactivity of Nanohydroxyapatite-Gelatin Paste as A Scaffold Using Simulated Body Fluid, *Journal of Carcinogenesis*, *Vol.24, No.2s*, 894-904

1. INTRODUCTION

Surgical procedures are used to replace, repair, or regenerate bone that has been damaged by infection, trauma, or another disease.[1] Many studies have demonstrated the effectiveness of tissue engineering in dental, periodontal, and craniofacial regeneration in terms of tissue repair and biological performance.[2], [3] Tissue engineering requires three critical components: stem cells, scaffolds, and signaling molecules or growth factors.[2], [3]

© 2025 Journal of Carcinogenesis | Published for Carcinogenesis Press by Wolters Kluwer-Medknow

Scaffolds function as an extracellular matrix and promote tissue regeneration.[3] Bone grafts are a common type of scaffold used in periodontal treatment and they are expected to have osteogenesis, osteoinductive, osteoconductive, or a combination of these properties.[1], [3] Autograft is the gold standard for bone grafting, but it has some drawbacks including pain, limited donor areas, and risk of infection.[1], [4], [5] Alloplastic has recently been used as a bone graft substitute for autograft due to its osteoinductive, osteoconductive, biocompatible, and bioactive properties in an unlimited quantity.[6] Previous research has also shown that patients experience less pain and discomfort when using alloplasts rather than autografts.[1], [4]

Alloplast as scaffolds are required to achieve stability between mechanical and biodegradation to facilitate the rapid development of new biomaterials, one of which is the development of nanomaterials like nanohydroxyapatite (nHA). Nanohydroxyapatite is a nanomaterial component of hydroxyapatite that serves as the mineral of human bone. [5], [7] Nanohydroxyapatite improves degradability while increasing osteoconductive, mechanical, and cell attachment properties.[7], [8]

The bioactivity of nanomaterials along with biocompatibility have an important role in serving as a scaffold in bone regeneration.[5], [9] The physical and chemical properties of materials influence their bioactivity. Soluble characteristics like pH and temperature have an impact on bioactivity.[9], [10] Kong et al, found that chitosan/ nHA had better bioactivity in SBF than chitosan alone.[11]

Nanohydroxyapatite has been formulated into many forms including paste to improve bioactivity. Pastes are minimally invasive forms that can simplify surgery and allow easy access to narrow and deep areas, such as periodontal tissue.[12], [13]

A matrix is required to turn nanohydroxyapatite into a paste, collagen is one of the most commonly used, but it can be difficult to obtain in some areas and is relatively expensive. Gelatin as an alternative to collagen has gained popularity due to its properties and low cost.[14] Gelatin is obtained by partial hydrolysis of collagen. In tissue engineering, gelatin is known to improve tissue repair because its structure promotes cell adhesion to create conditions similar to the extracellular matrix (ECM), it is biodegradable, and it is simple to manipulate during the gelation process.[3], [15]

The combination of gelatin and nHA was expected to produce a mixture that mimicked the structure of bones. Yadav and Srivastava discovered that hydroxyapatite and gelatin mixtures degrade faster than hydroxyapatite alone.[16] Using hydroxyapatite scaffolds and gelatin as nanocomposites, Barbani et al. showed a rise in osteogenic differentiation of the periodontal ligament in their study.[17]

This study aims to assess the bioactivity of nanohydroxyapatite gelatin paste as a scaffold using simulated body fluid, which used to treat irregular bone defects in bone regeneration therapy and to make the bone graft placement easier during surgery. The bioactivity of nanohydroxyapatite gelatin was assessed using pH, degradation, swelling, morphological characteristics with SEM, TEM, and EDS, chemical characteristics with FTIR after immersion in SBF in this research, and cell viability with the MTT assay. The findings of this research are expected to lay the groundwork for scaffold paste applications.

2. MATERIALS AND METHODS

Nanohydroxyapatite (nHA) was prepared by the National Research and Innovation Agency (BRIN, Indonesia), gelatin type B from bovine skin with 225 g Bloom (G9391 Sigma Aldrich, Germany), hydroxypropyl methylcellulose (HPMC, Sigma Aldrich, Germany), SBF was prepared by the Laboratory of Chemistry, Faculty of Medicine, Universitas Indonesia (Indonesia), using Kokubo's method. [18]

2.1 Transmission Electronic Microscope (TEM)

The nanostructure, morphology, and composition of nHA powder were examined using a Thermo Scientific Type FEI Tecnai G2 SuperTwin Transmission Electron Microscope at 200 kV. ImageJ software was used to measure the length and diameter of nHA powder obtained from TEM images at 29,000x magnification for morphological analysis and 71,000x magnification for diameter measurements. The measurements was repeated 8x.

2.2 Preparation of nHA/G Paste

A 20% gelatin solution was dissolved in distilled water using a stirrer at 40ºC for 30 min. The nHA from BRIN was mixed with a gelatin solution at a ratio of w/w (65/35; 60/40) for 15 min. HPMC was stirred at 60ºC for 15 min before adding to the nHA/gelatin mixture (nHA/G). The nHA/G pastes were stirred for 15 min with a stirrer at 40ºC. Table 1 displays the composition of each material.

© 2025 Journal of Carcinogenesis | Published for Carcinogenesis Press by Wolters Kluwer-Medknow

Table 1 Compositions of nHA/G paste

nHA/gelatin (weight ratio)	nHA (gram)	Gelatin (gram)	H_2O (ml)	HPMC (gram)	H_2O (ml)
65/35	9.285	5	20 ml	1	10
60/40	7.5	5	20 ml	1	10

2.3 Preparation of Simulated Body Fluid (SBF)

SBF was prepared following Kokubo's[18] guidelines, and stored at pH 7.4 and 37ºC. Table 2 compares the ions in SBF and human blood plasma.

Table 2 Comparison of ion concentration between simulated body fluid and human blood plasma

Concentration 10^{-3} mol	**Ion**							
	Na^+	**K^+**	**$Mg2^+$**	**Ca^{2+}**	**Cl^-**	**HCO_{3-}**	**HPO_4^{3-}**	**SO_4^{2-}**
SBF	142.0	5.0	1.5	2.5	147.8	4.2	1.0	0.5
Blood Plasma	142.0	5.0	1.5	2.5	103.0	27.0	1.0	0.5

2.4 Degradation and Swelling

A sample of nHA/G paste was placed in a round mold with a 6 x 3 mm diameter until it reached the desired setting. Samples were weighed using an analytical balance (W_0) and immersed in 10 ml of SBF solution with pH 7.4. Samples were incubated for 1, 2, 7, and 14 days at 37ºC (*Thermo Scientific*, Heratherm IMH60, USA).

After each incubation period, the SBF was removed with filter paper (d: 11 µm). The samples were then washed with distilled water, and filtered again with filter paper, and the wet weight was determined. Initial weight (W_0) and wet weight (Wt) are calculated to obtain the absorbency value (A) in the equation below:

$$\mathrm{A} = \frac{W_t - W_0}{W_o}\ x\ 100\%$$

After that, the sample was dried in a desiccator for 24 hours before being measured using analytical weight (W_1). The degradation ratio (Wn) was computed as follows:

$$\mathrm{Wn} = \frac{(W_0 - W_{1)} x\ 100\%}{W_o}$$

2.5 pH Analysis

The samples were incubated for 1, 2, 7, and 14 days, and kept at room temperature for 10 min. The pH of each sample was determined in triplicate using a calibrated pH meter (*Thermo Scientific,* Orion Star A211, USA).

2.6 Fourier Transform Infrared (FTIR)

The sample was analyzed using an FTIR Nicolet iS50, with a spectral range of 4000–400 cm−1 to detect absorption before SBF immersion, and 1, 2, 7, and 14 days after SBF immersion, the KBr pallet was used for the spectra. The analysis was done using OriginPro2023.

© 2025 Journal of Carcinogenesis | Published for Carcinogenesis Press by Wolters Kluwer-Medknow

2.7 SEM and EDS

The sample was tested using a 20 kV High Vacuum SEM FEI Quanta 650 ESEM at a scale of 30 µm. Morphological analysis of the scaffold surface was performed using ImageJ on an SEM Image at 1000x magnification, while pore measurements were performed on an SEM Image at 5000x magnification. The calcium and phosphorus compositions were determined using EDS integrated with SEM.

2.8 Cell Viability Test

The MC3T3-E1 cells were cultured using Dulbecco's Modified Eagle Medium (Sigma Aldrich, Germany) with 10% fetal bovine serum (Sigma Aldrich, Germany) in a 96-well plate for 24 h with cell concentration $1x10^5$/well. The nHA/G paste was then added to the cell culture and incubated for 1, 2, and 3 days. Following the incubation period, the MTT assay solution (3-(4,5-dimethylthiazol-2-yl)-2,5-diphenyltetrazolium bromide) (Sigma Aldrich, Germany) was added to all of the samples and incubated for 3.5 h. The unreacted dye was removed and 150 µl of acidified isopropanol was added to dissolve the intracellular purple formazan product to create a colored solution. The absorbance of this solution was measured using a spectrophotometer at 600 nm. All groups underwent three independent replications.

2.9 Statistical Analysis

IBM SPSS program version 22 was used to analyze numerical data. If a normal data distribution is present, a one-way ANOVA test can be utilized. If a non-normal data distribution is encountered, the Kruskal-Wallis test can be employed.

3. RESULTS

3.1 TEM Analysis

The nHA powder was examined under TEM to determine its morphology and particle shape. Fig. 1 depicts nHA crystals that were shaped like clumping and aggregating needles. The particles were porous and interconnected. (DIMINTA kasih prove karena menurut editor gambar ga kelihatan interconnected dan porous). The particles have an average length of 181.7 nm and a diameter of 26.9 nm.

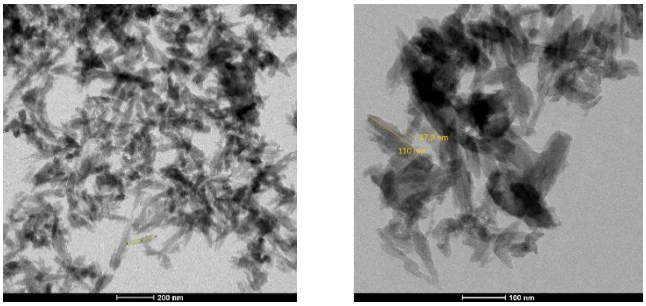

(a) (b)

Figure 1. (a) TEM image of nHA powder with magnification 29.000x (b) magnification 71.000x

3.2 Degradation and Swelling

The degradation rate of the nHA/G 65/35 and nHA/G 60/40 pastes increased steadily. The peaked on day 7 of immersion as shown in Fig. 2. Statistical analysis revealed a significant difference ($p < 0.05$) between nHA/G 65/35 and nHA/G 60/40 pastes after immersion in SBF on each immersion period. The swelling test revealed a significant difference in p-values of 0.000 between before and after immersion of pastes (Why is the difference in swelling between the pastas too big?). The absorbency of paste surfaces varied significantly between days 7 and 14.

© 2025 Journal of Carcinogenesis | Published for Carcinogenesis Press by Wolters Kluwer-Medknow

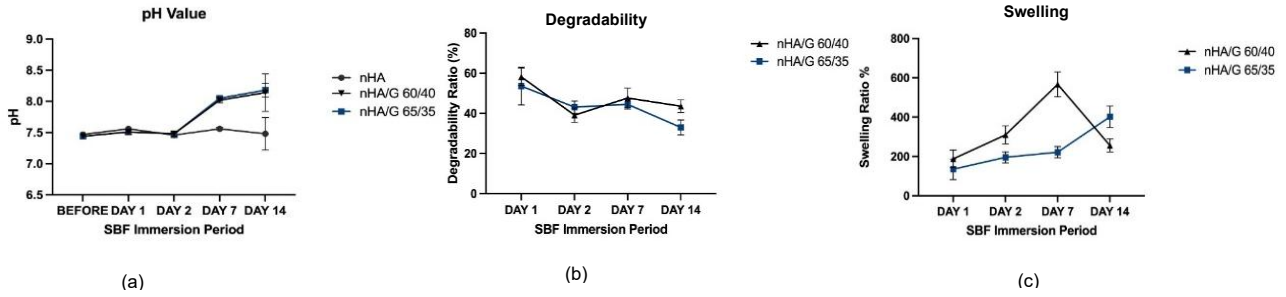

Figure 2. (a) pH Value nHA/G paste (b) Degradability rate (c) Swelling rate

3.3 pH Analysis

Figure 2 shows a comparison of pH at each immersion period for nHA/G 65/35 and 60/40 pastes. All samples' initial pH matched the SBF solution's pH, which is 7.4 at 37°C. Statistical analysis revealed a significant difference ($p < 0.05$) between nHA/G 65/35 and 60/40 pastes on days 1, 7, and 14 of immersion.

3.4 FTIR Analysis

In both pastes, the nHA spectrum revealed absorption peak bands of *v1* PO_4^{3-}, *v3*PO_4^{3-} , and CO_3^{2-}. The amide groups that indicated the presence of gelatin also identified functional groups like N-H, C=O, and O-H. There was no statistically significant difference between the two pastes.

The FTIR spectrum of nHA/G 65/35 shows the highest absorption value of the O-H functional group after 7 days of immersion at a wavelength of 3360 cm^{-1}. The highest absorption peaks of PO_4^{3-} bands were observed at respective wavelengths of 1415 cm^{-1}, 1020 cm^{-1}, and 558 cm^{-1} after 14 days of SBF immersion. Meanwhile, O-H bands in nHA/G 60/40 exhibited intense absorption peaks after 7 days of immersion at wavenumber 3358 cm^{-1}. Fig. 3 depicts the complete FTIR analysis.

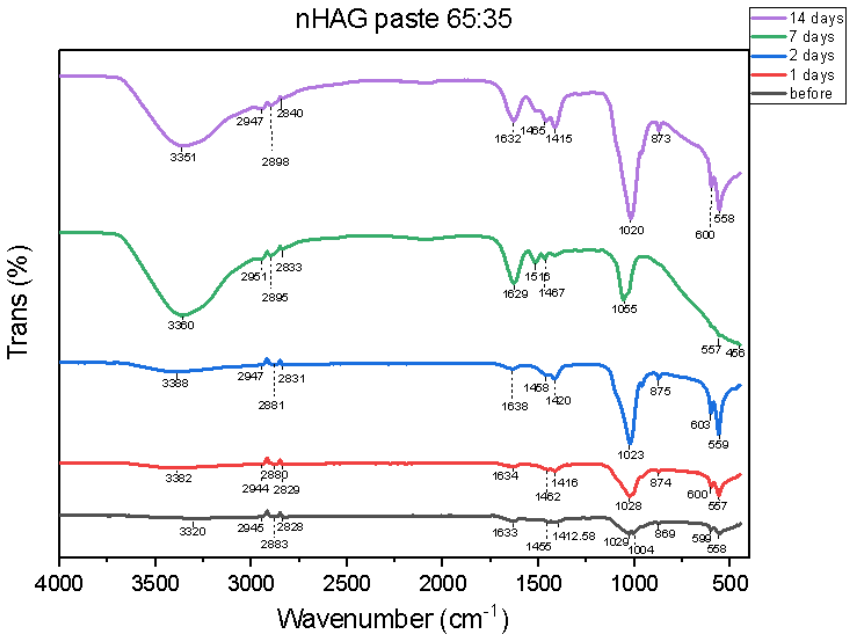

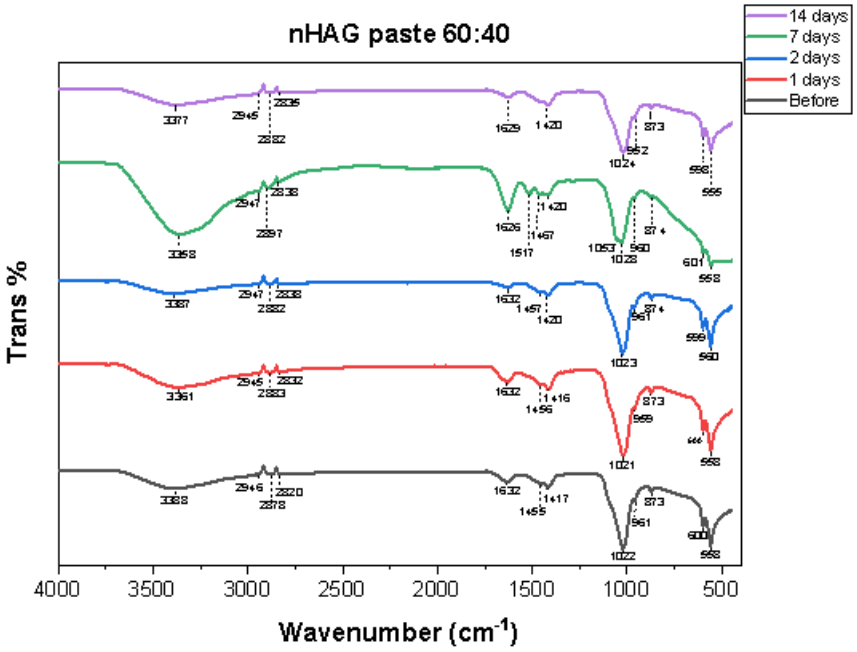

Figure 3. FTIR result of nHA/G paste

3.5 Morphological Analysis

The morphology of nhA 60/40 paste before and after 24h, 48h, and 7 days of immersion is irregularly coral-shaped with unclear boundaries, but after 14 days, the particles appear denser. NHA/G 65/35 paste has the same particle shape but with more defined boundaries. Particles stack on top of one another to form pores, whereas nHA/G 65/35 is more stratified to form pores (Fig 4). The SEM images were analyzed with ImageJ software, and nHA/G 65/35 (7.521) after 7 days of immersion. After immersion, nHA/G 60/40 had a larger pores diameter (9.145 ±4.343) on the 7th day, while nHA/G 65/35 was not unaffected NHA/G 65/35 after 7 days of immersion (69.9%).

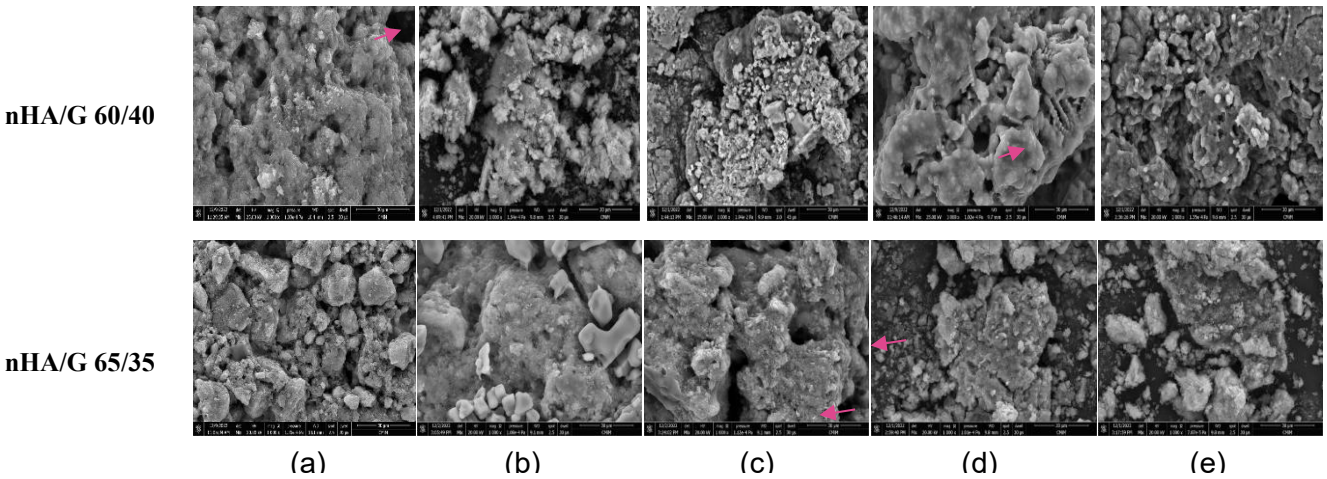

Figure 4. SEM overview of 1000x magnification nHA/G 60/40 and 65/35 paste (a) Before immersion (b) Day 1 (c) Day 2 (d) Day 7 (e) Day 14

The highest calcium and phosphorus composition in nHA/G 60/40 and nHA/G 65/35 were before immersion. The Ca/P ratio before and after immersion had a Ca/P ratio of > 1.67, indicating stoichiometric biological apatite.

3.6 Cell Viability

Cell viability was assessed in the nHA/G 65/35 and nHA/G 60/40 pastes after 1, 2, and 3 days. Cells cultured on top of both pastes indicated a percentage of survivability greater than 70%, with no significant difference between the two pastes. On days 2 and 3, the nHA/G 60/40 paste has a higher viability percentage than the nHA/G 65/35 paste (Fig. 5).

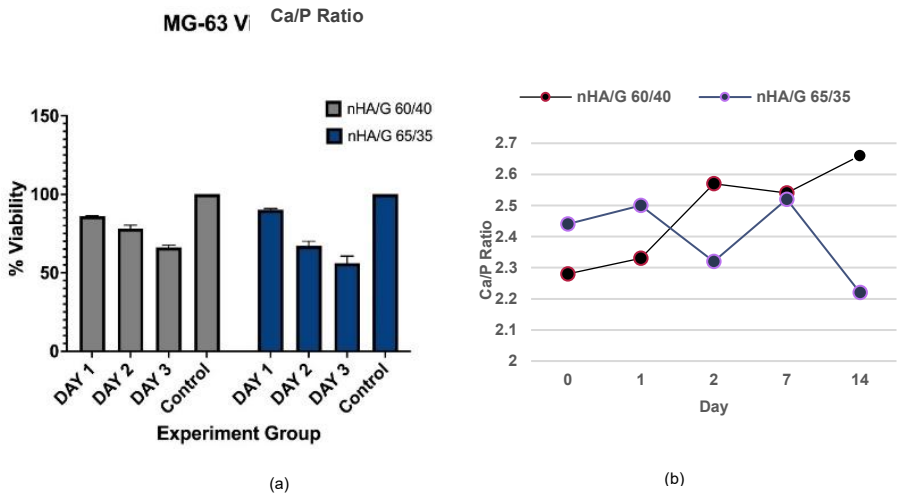

Figure 5. (a) Viability test with MTT assay (b) Ca/P Ratio

4. DISCUSSION

Bioactivity is a key biomaterial property for the ideal scaffold.[9], [10] In bone, bioactivity occurs when an apatite layer forms due to the presence of $PO_4^{3-}$and Ca^{2+} ions.[19] The bioactivity can be determined by examining the chemical properties, pH, morphology, and temperature of the biomaterial when it comes into contact with bodily fluids, such as the SBF solution.[9], [20]

Kokubo devised a test that uses simulated body fluid (SBF) to determine the bioactivity of biomaterial. Simulated body fluid is a substance with blood plasma-like concentrations that have been shown to accurately represent tissues, as evidenced by studies on glass-ceramic materials which discovered that an apatite layer forms on SBF immersion and on bone in vivo.[18]

The nHA/G 60/40 paste FTIR detected the highest absorption intensity of the PO_4^{3-} functional group on the 7th day after immersion, but the highest pH occurred on the 14th day (8.14) of immersion. It is believed that various factors, including contamination during the incubation phase and paste form, can influence pH by increasing the reactivity of SBF.[21] Chong et al's study, which used modified nHA and polysaccharide pastes also found that pH decreased as the apatite layer developed.[22]

Meanwhile, nHA/G 65/35 demonstrated the greatest of pH increase (8.14) as evidenced by the 14th day FTIR that results which revealed the highest absorption intensity of the PO_4^{3-} functional group.[23] Galow et al studied the osteoblast-like cell line MC3T3-E1 for 14 days at various pH levels, and the results showed that osteoblast activity was increased and osteoclast activity was inhibited at a pH close to alkaline (8.4).[24] Alkaline pH can increase Ca and P ion formation, resulting in more PO_4^{3-} and bioactivity, it also helps the injectable paste set in the bone.[22], [23]

Alkaline pH which promotes positive ion (proton) exchange, increases the degradability of inorganic nanostructures such as nHA.[23] Until day seven of the study, the increase in pH was consistent with swelling and degradation; however, by day fourteen, the increase in pH did not correspond to a decrease in degradation. Degradation is necessary to regulate the rate of bone formation.[25] The situation in this study is also confirmed by increased absorption of the O-H functional groups in FTIR, which demonstrates the biomaterial's hydrolysis. Both pastes showed absorption peaks for O-H bands on the 7th day of immersion.

The gelatin in the paste also promotes O-H hydrolysis, increasing the degradation rate, which is consistent with the findings of this study.[14] Gelatin has a three-dimensional structure that binds nHA particles, according to Chen et al.'s research on nHA/G nanocomposites, this structure decomposes quickly, causing nHa to be released more quickly and increasing degrading power.[15] The combination of HPMC also helps to increase the degradability of nHA. Hydrophilic polymers such as HPMC degrade rapidly in water. Zeeshan et al discovered that HPMC can degrade in a PBS system, affecting the rate at which scaffolds degrade.[26]

Gelatin content in the pastes also influenced swelling because gelatin helps to maintain the paste's colloidal system. Gelatin

will release liquid at high temperatures while absorbing liquid at low temperatures. The absorbed fluid causes swelling of the cell pore, which facilitates cell infiltration into the scaffold. The high absorbency of the scaffold fluid enables cell bioactivity.[27], [28] However, high water absorption can cause the scaffold to separate from the planting site and retract material due to excessive swelling.[28] The formation of a hydroxyapatite layer during the immersion period increases the number of pores and absorption, as demonstrated in nHA/G 65/35. The increased absorption of PO_4^{3-} observed on FTIR, after immersion indicated the formation of crystalline apatite layers. This occurs as a result of Ca^{2+} from SBF binding to OH- and PO_4^{3-} on the surface of the matrix on apatite to form a hydroxyapatite layer, as demonstrated in nHA/G 65/ 35 with the highest absorption peaks 14 days after immersion.[29]It was also supported by an EDS test, which revealed that the Ca/P ratio of nHA/G 65/35 reached 2.66 after 14 days of immersion, indicating the formation of the same apatite layer as the natural bone-forming structure (Ca/P ratio > 1.67).[25], [30]

The Ca/P ratio value of nHA/G 65/35 is higher than that of others due to its high nanohydroxyapatite composition, indicating high hydroxyapatite layer formation. The formation of a high hydroxyapatite layer promotes cell bioactivity because it has conductive properties for collagen and fibronectin attachment; increasing osteoblast adhesion and mineralization while also forming bonds between the scaffold material and surrounding bone tissue.[25], [27], [30] According to Cortéz et al, apatite crystals appeared on the surface of CoCrMO with a bed of wollastonite, bioactive glass, and HA after 7 days of SBF immersion, followed by a homogeneous apatite layer after longer immersion times.[31] After immersion, OH^- and PO_4^{3-} not only attract calcium, but also other minor elements, like sodium, magnesium, and chlorine.[25], [32] This is evident by the detection of other minor elements following a brief immersion in the SBF solution.

The condition of decreased of calcium and phosphorus ions after immersion can also be caused by releasing these ions, which are attracted by ions in the SBF solution, a process known as reprecipitation. Hydrolysis is the process of exchanging ions or breaking chemical molecular bonds between the solid and liquid phases. [33], [34] This situation may lead to degradation.

Cells can infiltrate the scaffold because the pores are larger than their size.[35], [36] There is no precise pore size value of the scaffold, but 100–400 μm is ideal for fibroblast cell perforation measuring 186–200 μm, meanwhile, chondrocytes and osteoblasts measuring 380–405 μm.[37] This study found that the average pore size of nHA powder (245 μm), nHA/G 60/40 (344.1 μm), and nHA/G 65/35 (446.9 μm) was larger than that of fibroblast cells (186 μm). nHA/G 65/35 had larger pores than the others.

The nHA/G 65/35 pore size was large with a high calcium and phosphorous composition. These differences in pore size were influenced by the concentration of gelatin in the pastes. Pastes containing a high concentration of gelatin increase the material's porosity. A high gelatin concentration reduces the viscosity of the pastes, resulting in large and multiple pores. Another factor that can influence the size of this pore is the duration of immersion in the SBF solution.[37] Previous research has shown that long immersion in SBF solution causes several apatite particles to form in the scaffold, with the accumulated layers forming 3-dimensional pores.[32], [38] Meanwhile, nHA powder's description matches the Rahman et al study, with a needle-like shape that appears to agglomerate and interconnected structures. The length of nHA powder in this study exceeded 100 nm and its diameter exceeded 2 nm. This demonstrates that the particle size remains within the range of nanometer grade and has a good dispersive property in polymers, which has a positive effect on biological properties as a scaffold.

Consistent with this study's finding, Yang et al. also reported a smaller size of crystallite nHA when CO_3^{2-} ions were increasing. They evaluate two possible mechanisms for the existence of CO_3^{2-}: (1) a direct substitute of O-H by CO_3^{2-} in the hydroxyapatite structure, known as a type-A substitution; and (2) a substitute of PO_4^{3} tetrahedral groups by CO_3^{2-}, known as type-B substitution.[39] Due to its ionic composition and physiological characteristics promoting bone formation, CO_3^{2-} is important in bone metabolism.[39] For a viability test using the MTT assay, this study also used the osteoblast-like cell line MC3T3-E1, which revealed that both pastes are nontoxic after incubation on day 3. Mild cytotoxicity is defined as having a viability percentage of 60% to 90%.[40]

This study's limitation is that no examinations were carried out to identify the composition of the apatite layer that developed on the biomaterial's surface. Furthermore, the apatite layer's creation on SBF has several limits and is merely a preliminary sign of a biomaterial's potential; as such, it cannot alter the degree of accuracy of cell research conducted in vitro. Furthermore, a cellular bioactivity test is necessary.

5. CONCLUSION

In this study, the nHA/G 65/35 paste is the best candidate for use as a scaffold due to its superior bioactivity in terms of degradability, pH, and physical, and chemical properties. It is also conducive to cell growth; with ideal surface morphological properties, a high calcium-phosphorus ratio, and optimal absorption. Further research into the development of nHA/G pastes is required, including immunological tests, in vivo tests, and stored-time tests.

© 2025 Journal of Carcinogenesis | Published for Carcinogenesis Press by Wolters Kluwer-Medknow

Funding Statement

This study was supported by a grant from the Directorate of Research and Community Engagement Universitas Indonesia (PUTI Grant Scheme No: NKB-616/UN2.RST/HKP.05.00/2022).

Data Availability Statement

Data available with the paper or supplementary information:

The authors declare that the data supporting the study's findings are available in the paper and supplementary information files. If any raw data files are required in another format they can be obtained from the corresponding author upon reasonable request. Source data are provided in this paper.

Acknowledgments

Prof. Akihiko Tanimura, Ph.D., Department of Pharmacology, School of Dentistry, Health Science University of Hokkaido for the generous gift of MC3T3-E1.

Declarations Of Conflicting Interests

The authors declare that there is no conflict of interest.

REFERENCES

[1] R. Zhao, R. Yang, P. R. Cooper, Z. Khurshid, A. Shavandi, and J. Ratnayake, "Bone grafts and substitutes in dentistry: A review of current trends and developments," Molecules, vol. 26, no. 10, pp. 1–27, 2021, doi: 10.3390/molecules26103007.

[2] S. Raveau and F. Jordana, "Tissue Engineering and Three-Dimensional Printing in Periodontal Regeneration : A Literature Review," J Clin Med., vol. 9, no. 12, p. 4008, 2020.

[3] B. Chang, N. Ahuja, C. Ma, and X. Liu, "Injectable scaffolds: Preparation and application in dental and craniofacial regeneration," Materials Science and Engineering R: Reports, vol. 111, pp. 1–26, 2017, doi: 10.1016/j.mser.2016.11.001.

[4] C. Bucchi, M. Fabbro, A. Arias, J. M. Mendes, and M. Ordonneau, "Multicenter study of patients ' preferences and concerns regarding the origin of bone grafts utilized in dentistry," Patient preference and adherence, no. 13, pp. 179–185, 2019.

[5] A. Hatami et al., "Hydroxyapatites and nano-hydroxyapatites as scaffolds in drug delivery towards efficient bone regeneration : A review," Carbohydrate Polymer Technologies and Applications, vol. 9, no. January, p. 100692, 2025, doi: 10.1016/j.carpta.2025.100692.

[6] S. Fukuba, M. Okada, K. Nohara, and T. Iwata, "Alloplastic bone substitutes for periodontal and bone regeneration in dentistry: Current status and prospects," Materials, vol. 14, no. 5, pp. 1–28, 2021, doi: 10.3390/ma14051096.

[7] F. Zakaria;Yang;Janses;Othman;Zein, "Nanophase Hydroxyapatite as a Biomaterial in Advanced Hard Tissue Engineering : A Review," Tissue engineering. Part B, Reviews, vol. 19, no. 5, pp. 431–441, 2013, doi: 10.1089/ten.teb.2012.0624.

[8] J. S. Lee et al., "In vivo study of chitosan-natural nano hydroxyapatite scaffolds for bone tissue regeneration," International Journal of Biological Macromolecules, vol. 67, pp. 360–366, 2014, doi: 10.1016/j.ijbiomac.2014.03.053.

[9] A. Dridi, K. Zlaoui, and S. Somrani, "Journal of Physics and Chemistry of Solids Mechanism of apatite formation on a poorly crystallized calcium phosphate in a simulated body fluid (SBF) at 37 ◦ C," Journal of Physics and Chemistry of Solids, vol. 156, no. April, p. 110122, 2021, doi: 10.1016/j.jpcs.2021.110122.

[10] M. Omidi et al., 7. Characterization of biomaterials. Elsevier Ltd, 2017. doi: 10.1016/B978-0-08-100961-1.00007-4.

[11] L. Kong, Y. Gao, G. Lu, Y. Gong, N. Zhao, and X. Zhang, "A study on the bioactivity of chitosan/nano-hydroxyapatite composite scaffolds for bone tissue engineering," European Polymer Journal, vol. 42, no. 12, pp. 3171–3179, 2006, doi: 10.1016/j.eurpolymj.2006.08.009.

[12] D. B. Lima, R. D. Almeida, M. Pasquali, S. P. Borges, M. L. Fook, and H. M. Lisboa, "Physical characterization and modeling of chitosan/peg blends for injectable scaffolds," Carbohydrate Polymers, vol. 189, pp. 238–249, 2018, doi: 10.1016/j.carbpol.2018.02.045.

[13] H. Kaneko, Aoi; Marukawa, Eriko ;Harada, "Hydroxyapatite Nanoparticles as Injectable Bone Substitute Material in a Vertical Bone Augmentation Model," in vivo, vol. 1061, no. 34, pp. 1053–1061, 2020, doi: 10.21873/invivo.11875.

© 2025 Journal of Carcinogenesis | Published for Carcinogenesis Press by Wolters Kluwer-Medknow

[14] C. Fang et al., "Metformin-Incorporated Gelatin / Nano-Hydroxyapatite Scaffolds Promotes Bone Regeneration in Critical Size Rat Alveolar Bone Defect Model," Int J Mol Sci, vol. 23, no. 1, p. 558, 2022.

[15] X. Chen, D. Wu, J. Xu, T. Yan, and Q. Chen, "Gelatin / Gelatin-modified nano hydroxyapatite composite scaffolds with hollow channel arrays prepared by extrusion molding for bone tissue engineering," Marer. Res.express, vol. 8, p. 010527, 2021.

[16] N. Yadav and P. Srivastava, "In vitro studies on gelatin / hydroxyapatite composite modi fi ed with osteoblast for bone bioengineering," Heliyon, vol. 5, no. 5, p. e01633, 2019, doi: 10.1016/j.heliyon.2019.e01633.

[17] N. Barbani et al., "Hydroxyapatite/gelatin/gellan sponges as nanocomposite scaffolds for bone reconstruction," Journal of Materials Science: Materials in Medicine, vol. 23, no. 1, pp. 51–61, 2012, doi: 10.1007/s10856-011-4505-2.

[18] T. Kokubo and S. Yamaguchi, "Simulated body fluid and the novel bioactive materials derived from it," Journal of Biomedical Materials Research - Part A, vol. 107, no. 5, pp. 968–977, 2019, doi: 10.1002/jbm.a.36620.

[19] D. Tsiourvas, A. Sapalidis, and T. Papadopoulos, "Hydroxyapatite/chitosan-based porous three-dimensional scaffolds with complex geometries," Materials Today Communications, vol. 7, pp. 59–66, 2016, doi: 10.1016/j.mtcomm.2016.03.006.

[20] O. Adamopoulos and T. Papadopoulos, "Nanostructured bioceramics for maxillofacial applications," Journal of Materials Science: Materials in Medicine, vol. 18, no. 8, pp. 1587–1597, 2007, doi: 10.1007/s10856-007-3041-6.

[21] B. F. Fiume E, Migneco C, Verné E, "Comparison Between Bioactive Sol-Gel and Melt-Derived Glasses/Glass-Ceramics Based on the Multicomponent SiO2-P2O5-CaO-MgO-Na2O-K2O System," Materials (Basel)., vol. 13, no. 3, p. 540, 2020.

[22] B. Chong et al., "Dielectric and biodegradation properties of biodegradable nano-hydroxyapatite / starch bone scaffold," Journal of Materials Research and Technology, vol. 18, pp. 3215–3226, 2022, doi: 10.1016/j.jmrt.2022.04.014.

[23] H. Miyajima, H. Touji, and K. Iijima, "Hydroxyapatite Particles from Simulated Body Fluids with Different pH and Their Effects on Mesenchymal Stem Cells," Nanomaterials (Basel), vol. 11, no. 10, p. 2517, 2021.

[24] A. M. Galow, A. Rebl, D. Koczan, S. M. Bonk, W. Baumann, and J. Gimsa, "Increased osteoblast viability at alkaline pH in vitro provides a new perspective on bone regeneration," Biochemistry and Biophysics Reports, vol. 10, pp. 17–25, 2017, doi: 10.1016/j.bbrep.2017.02.001.

[25] S. C. Wu, H. C. Hsu, S. K. Hsu, W. H. Wang, and W. F. Ho, "Preparation and characterization of four different compositions of calcium phosphate scaffolds for bone tissue engineering," Materials Characterization, vol. 62, no. 5, pp. 526–534, 2011, doi: 10.1016/j.matchar.2011.03.014.

[26] R. Zeeshan et al., "Hydroxypropylmethyl cellulose (HPMC) crosslinked Chitosan (CH) based scaffolds containing Bioactive glass (BG) and Zinc oxide (ZnO) for Alveolar Bone Repair," Carbohydrate Polymers, vol. 193, pp. 9–18, 2018, doi: 10.1016/j.carbpol.2018.03.046.

[27] M. Araújo, M. Miola, G. Baldi, J. Perez, and E. Verné, "Bioactive glasses with low Ca/P ratio and enhanced bioactivity," Materials, vol. 9, no. 4, 2016, doi: 10.3390/ma9040226.

[28] H. H. Lu, A. Tang, S. C. Oh, J. P. Spalazzi, and K. Dionisio, "Compositional effects on the formation of a calcium phosphate layer and the response of osteoblast-like cells on polymer-bioactive glass composites," Biomaterials, vol. 26, no. 32, pp. 6323–6334, 2005, doi: 10.1016/j.biomaterials.2005.04.005.

[29] P. N. Chavan, M. M. Bahir, R. U. Mene, M. P. Mahabole, and R. S. Khairnar, "Study of nanobiomaterial hydroxyapatite in simulated body fluid: Formation and growth of apatite," Materials Science and Engineering B: Solid-State Materials for Advanced Technology, vol. 168, no. 1, pp. 224–230, 2010, doi: 10.1016/j.mseb.2009.11.012.

[30] S. Shahi, S. Sharifi, R. Khalilov, S. M. Dizaj, and E. D. Abdolahinia, "Gelatin-hydroxyapatite Fibrous Nanocomposite for Regenerative Dentistry and bone Tissue Engineering," The Open Dentistry Journal, vol. 16, no. 1, pp. 1–10, 2022, doi: 10.2174/18742106-v16-e2208200.

[31] D. A. Cortés, A. Medina, S. Escobedo, and M. A. López, "Biomimetic apatite formation on a CoCrMo alloy by using wollastonite, bioactive glass or hydroxyapatite," Journal of Materials Science, vol. 40, no. 13, pp. 3509–3515, 2005, doi: 10.1007/s10853-005-2856-0.

[32] C. Kailasanathan and N. Selvakumar, "Comparative study of hydroxyapatite/gelatin composites reinforced with bio-inert ceramic particles," Ceramics International, vol. 38, no. 5, pp. 3569–3582, 2012, doi: 10.1016/j.ceramint.2011.12.073.

© 2025 Journal of Carcinogenesis | Published for Carcinogenesis Press by Wolters Kluwer-Medknow

[33] C. I. Degradable, M. Treiser, S. Abramson, and R. Langer, Definitions Relating to The Process of degradation Versus Biodegradation, And Erosion Versus Bioerosion, Third Edit., no. 2008. Elsevier, 2010. doi: 10.1016/B978-0-08-087780-8.00021-8.

[34] N. L. Davison, F. B. Groot, and D. W. Grijpma, Degradation of Biomaterials, Second Edi. Elsevier Inc., 2015. doi: 10.1016/B978-0-12-420145-3.00006-7.

[35] H. Lian, L. Zhang, and Z. Meng, "Biomimetic hydroxyapatite/gelatin composites for bone tissue regeneration: Fabrication, characterization, and osteogenic differentiation in vitro," Materials and Design, vol. 156, pp. 381–388, 2018, doi: 10.1016/j.matdes.2018.07.009.

[36] A. Bigi, S. Panzavolta, and N. Roveri, "Hydroxyapatite-gelatin films: A structural and mechanical characterization," Biomaterials, vol. 19, no. 7–9, pp. 739–744, 1998, doi: 10.1016/S0142-9612(97)00194-4.

[37] M. C. Chang, C. C. Ko, and W. H. Douglas, "Preparation of hydroxyapatite-gelatin nanocomposite," Biomaterials, vol. 24, no. 17, pp. 2853–2862, 2003, doi: 10.1016/S0142-9612(03)00115-7.

[38] F. Verisqa, S. Triaminingsih, and J. E. M. Corputty, "Composition of chitosan-hydroxyapatite-collagen composite scaffold evaluation after simulated body fluid immersion as reconstruction material," Journal of Physics: Conference Series, vol. 884, no. 1, pp. 6–11, 2017, doi: 10.1088/1742-6596/884/1/012035.

[39] W. H. Yang, X. F. Xi, J. F. Li, and K. Y. Cai, "Comparison of crystal structure between carbonated hydroxyapatite and natural bone apatite with theoretical calculation," Asian Journal of Chemistry, vol. 25, no. 7, pp. 3673–3678, 2013, doi: 10.14233/ajchem.2013.13709.

[40] A. M. Lopera-echavarría, D. Medrano-david, A. M. Lema-perez, P. Araque-marín, and M. E. Londo, "In vitro evaluation of confinement , bioactivity , and degradation of a putty type bone substitute," vol. 26, no. September 2020, 2021, doi: 10.1016/j.mtcomm.2021.102105.

© 2025 Journal of Carcinogenesis | Published for Carcinogenesis Press by Wolters Kluwer-Medknow